Metabolic Brain Disease (2025) 40:201
https://doi.org/10.1007/s11011-025-01613-x

RESEARCH

LncRNA MEG3 promotes pyroptosis via miR-145-5p/TLR4/NLRP3 axis and aggravates cerebral ischemia-reperfusion injury

Lei Li[1] · Hao Zha[2] · Wei Miao[1] · Chunyan Li[1] · Aimei Wang[1] · Shiyuan Qin[1] et al. ***[full author details at the end of the article]***

Received: 20 December 2024 / Accepted: 11 April 2025

Abstract

Long noncoding RNA (lncRNA) MEG3 has been considered as a novel target for alleviating the brain tissue damage during cerebral ischemia-reperfusion injury (CIRI). Numerous studies have reported that pyroptosis is involved in the pathogenesis of CIRI. This study focused on whether MEG3 modulates CIRI via pyroptosis and its underlying mechanism. The middle cerebral artery occlusion/reperfusion (MCAO/R) mouse model and the oxygen glucose deprivation/reoxygenation (OGD/R) cell model were established. si-MEG3 and miR-145-5p inhibitor were transfected to inhibit MEG3 and miR-145-5p, respectively. As a TLR4 inhibitor, Resatorvid inhibits the TLR4 signaling pathway. TTC and TUNEL staining were used for infarction volume and cell death detection. The differential expression of MGE3, miR-145-5p, TLR4, NLRP3, Caspase-1, IL-1β, and IL-18 was determined using real-time PCR and western blot. The interaction between MEG3 and miR-145-5p, as well as between miR-145-5p and TLR4 was confirmed by the dual-luciferase reporter assay. This study confirmed that the elevated expression of MEG3 during CIRI, and it contributes to pyroptosis by regulating miR-145-5p/TLR4 axis. The knockdown of MEG3 reduced the expression of TLR4, NLRP3, Caspase-1, IL-1β, and IL-18, thereby preventing pyroptosis. Inhibition of miR-145-5p reversed the effect of MEG3 knockdown and promoted pyroptosis. Resatorvid, the inhibitor of TLR4, counteracted the effect of miR-145-5p inhibitor and suppressed pyroptosis. Our findings reveal that MEG3 promotes pyroptosis via miR-145-5p/TLR4/NLRP3 axis and aggravates CIRI, suggesting a potential therapeutic target for ischemic stroke.

Extended author information available on the last page of the article

Published online: 13 May 2025

Graphical abstract

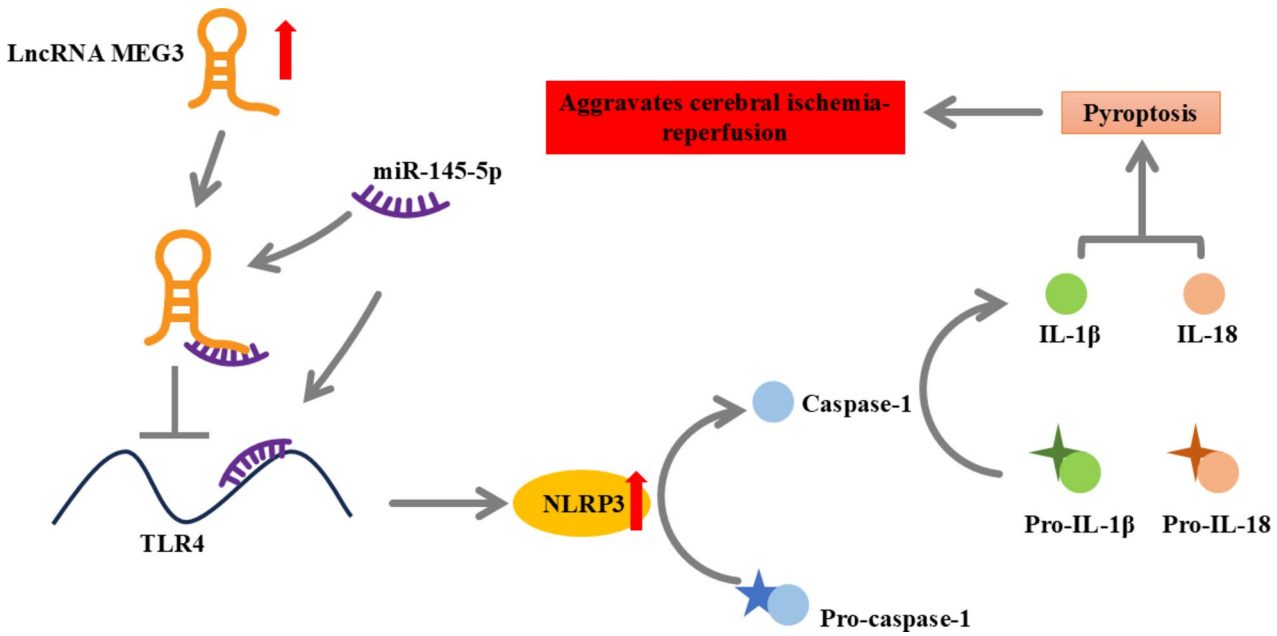

Keywords Cerebral ischemia-reperfusion injury · Long noncoding RNA MEG3 · MiR-145-5p · TLR4 · Pyroptosis

Introduction

Stroke includes both hemorrhagic stroke and ischemic stroke, with ischemic stroke accounting for about 87% of all strokes (Bailey et al. 2012). The main causes of ischemic stroke include the formation of atheromatous plaque, cardiogenic cerebral infarction, and cerebral small-vessel disease (CSVD) (Jean et al. 1998). The methods for managing ischemic stroke include intravenous thrombolysis (IVT) or intra-arterial thrombolysis (IAT), which may carry the risk of reperfusion injury. Reperfusion injury refers to the cellular injury and dysfunction caused by the immediate disruption of cellular metabolism and ion balance following the restoration of blood flow in ischemic tissue. In the case of cerebral ischemia-reperfusion injury (CIRI), when the blocked blood vessels are reopened, a large amount of oxygen and nutrients suddenly flow into the previously ischemic brain tissues. This flux may lead to the destruction of cell membranes, dysfunction of organelles, an overload of intracellular calcium ions, and subsequently cause cell swelling, necrosis, and apoptosis (Xiong et al. 2019). It is crucial to identify novel targets that can mitigate CIRI in order to salvage the brain tissue damaged during reperfusion.

Long non-coding RNA (lncRNA) refers to a type of RNA that is lengthy and does not code for proteins. They are characterized by high specificity and differential stability (Xiong et al. 2019), operating through interference with transcription and translation (Quek et al. 2015), maintaining mRNA stability (Shuman 2020), and influencing DNA and protein activity (Wu et al. 2022b; Zhu et al. 2013). They are being investigated as potential biomarkers and therapeutic targets for diseases such as cancers, cardiovascular ailments, diabetes, and neurological disorders. Recently, more and more attention has been paid to LncRNA MEG3 as a promising target in CIRI. In the oxygen glucose deprivation/reoxygenation (OGD/R) cell model and middle cerebral artery occlusion/reperfusion (MCAO/R) mice model, MEG3 is significantly up-regulated. It promotes CIRI by modulating oxidative stress and mitochondrial dysfunction (Yao et al. 2024), regulating microglial polarization (Li et al. 2020), and inducing pyroptosis (Liang et al. 2020) or apoptosis (Liu et al. 2016). But the specific molecular mechanisms involved need to be further investigated.

LncRNAs function as precursors and hosts of miRNAs, acting as competing endogenous RNAs (ceRNAs) that directly or indirectly influence miRNAs through competitive binding or sponge effects. miRNA has potential therapeutic effects in various diseases (Selvakumar et al. 2023, 2024; Preethi and Sekar 2021). In CIRI, miRNAs play a vital role in processes including oxidative stress, inflammation, and cell death. lncRNA C2 dat2 promotes autophagy and apoptosis induced by CIRI, and it acts as a ceRNA to negatively regulate miR-30d-5p expression (Xu et al. 2021). LncRNA CEBPA-AS1 alleviates CIRI by sponging miR-340-5p (Tu

et al. 2022). In the OGD/R cell model and MCAO/R mice model, the expression of LncRNA MALAT1 was significantly increased and it promotes CIRI through regulating miR-145 (Shi et al. 2020). This study aims to investigate how MEG3, as a ceRNA, regulates its downstream targets to exacerbate cerebral ischemia-reperfusion injury.

Inflammation is a significant contributor to brain injury following CIRI (Xiang et al. 2020). Toll-like receptor 4 (TLR4) is one of the crucial signaling modulators that regulate the inflammatory response (Winters et al. 2013), serving as a trigger for the pro-inflammatory process in ischemic stroke. In CIRI, microglial cells become activated and generate TLR4. TLR4 then recruits downstream signaling molecules, such as myeloid differentiation factor 88 (MyD88), to facilitate the nuclear translocation of NF-κB, leading to up-regulated transcription of inflammasome-related components, including inactive NLRP3, proIL-1β, and proIL-18 (Shao et al. 2015; Wang et al. 2013). Subsequent stimuli activate the NLRP3 inflammasome, which recruits and activates Caspase-1. Activated Caspase-1 cleaves gasdermin D (GSDMD) and promotes the maturation of IL-1β and IL-18 (Yu et al. 2020), thus inducing pro-inflammatory programmed necrosis-pyroptosis (Cookson and Brennan 2001). This suggests that TLR4 activated NLRP3 mediated cell pyroptosis plays an important role in cerebral ischemia-reperfusion injury. And a study has reported that lncRNA MEG3 triggers inflammatory responses in microglia by modulating the expression of NLRP3 via miR-7a-5p (Meng et al. 2021). Moreover, many studies have reported that NLRP3-mediated pyroptosis is involved in the pathogenesis of CIRI (Chen et al. 2023; Shi et al. 2023). Our research focuses on how MEG3, as a ceRNA, regulates downstream targets, thereby modulating NLRP3-mediated pyroptosis and exacerbating cerebral ischemia-reperfusion injury. We hope to provide a potential target for the treatment of CIRI.

Materials and methods

Animals and groups

Male SD rats (6–8 months, 280–320 g) were purchased from Beijing SiPeiFu. Rats were kept in a controlled environment with a 12-hour light/dark cycle, a temperature of 25 °C, 60% relative humidity, a noise level below 85 dB, and ventilation occurring 8–12 times per hour. Free access to food and water was offered. This work was approved by the Laboratory Animal Ethics Committee of Yunnan Luoyu Biological Technology Co., Ltd. Animal suffering was minimized. In this study, 42 SD rats were randomly assigned to 7 equal groups. The first stage of the study involved three groups, which were labeled as the Sham group, the MCAO 2h/R group, and the MCAO 4.5h/R group, respectively. MCAO/R were induced following the steps of MCAO/R induction. Rats in the MCAO 2h/R and MCAO 4.5h/R groups were treated with 2- or 4.5-hour occlusion, respectively. Rats from the Sham group underwent the same surgical procedures as the MCAO 2h/R and MCAO 4.5h/R groups except for the occlusion. The second stage of the study divided rats into five groups: the NC group, the MCAO 4.5h/R group, the si-MEG3+MCAO 4.5h/R group, the si-MEG3+miR-145-5p inhibitors+ MCAO 4.5h/R group, and the si-MEG3+miR-145-5p inhibitors+ MCAO 4.5h/R+Resatorvid group. All groups except the NC group received 4.5-hour occlusion and 48-hour reperfusion. Rats in the si-MEG3+MCAO 4.5h/R group were transfected with si-MEG3. The si-MEG3+miR-145-5p inhibitors +MCAO 4.5h/R group and the si-MEG3+miR-145-5p inhibitors+MCAO 4.5h/R+Resatorvid group were co-transfected with si-MEG3 and miR-145-5p inhibitors. And the si-MEG3+miR-145-5p inhibitors+ MCAO 4.5h/R+Resatorvid group were also administered Resatorvid (TAK- 242, TLR4 inhibitors) (5 mg/kg) once a day for 5 days. This study was conducted in accordance with the guiding principles of the Declaration of Helsinki and was approved by the Ethics Committee of the Second Affiliated Hospital of Kunming Medical University (protocol code: Audit-PJ-Ko-2022 - 124, approval date: May 5, 2022) and the Laboratory Animal Ethics Committee of Yunnan Luoyu Biotechnology Co Ltd (protocol code: SL20230410, Approval date: April 5, 2023).

MCAO/R induction

Anesthesia for rats was induced by intraperitoneal administration of 0.5 mg/kg sodium pentobarbital. Subsequently, ligate the proximal end of the right common carotid artery (CCA) and at the root of the external carotid artery (ECA) with 3 − 0 silk suture. The end of the internal carotid artery (ICA) was temporarily occluded with a microvascular clip. Then, a small incision was made on CCA. Then, a silicone-coated nylon filament was inserted into the ICA through the incision and reach the middle cerebral artery (MCA). After 2- or 4.5-hour occlusion, the filament was taken out to allow reperfusion.

Cell culture and groups

Mouse Hippocampal Neuronal Cell Line HT22 was maintained in DMEM medium (10% FBS and 1% (w/v) penicillin-streptomycin) and cultured in an incubator (37 °C, 5% CO_2) for further experimentation. Firstly, HT22 cells were divided into 5 groups: NC, OGD 2h/R, OGD 2h/R+si-MEG3, OGD 4.5h/R, and OGD 4.5h/R+si-MEG3. Cells in the OGD 2h/R+si-MEG3 and OGD 4.5h/R+si-MEG3

groups were transfected with si-MEG3. The NC group was transfected with the Negative control of siRNA. Cells in the OGD 2h/R, OGD 2 h/R+si-MEG3, OGD 4.5h/R, and OGD 4.5h/R+si-MEG3 groups were subjected to oxygen-glucose deprivation (OGD) for the indicated time. Secondly, cells were organized into the NC, OGD 2h/R, OGD 2h/R+miR-145-5p inhibitors, OGD 4.5h/R, OGD 4.5h/R+miR-145-5p inhibitors groups. The OGD 2h/R+miR-145-5p inhibitors and OGD 4.5h/R+miR-145-5p inhibitors groups were transfected with miR-145-5p inhibitors, and the NC group was transfected NC-inhibitors. Moreover, HT22 cells were divided into the NC, OGD 4.5h/R, OGD 4.5h/R+si-MEG3, OGD 4.5h/R+si-MEG3+miR-145-5p inhibitors, and OGD 4.5h/R+si-MEG3+miR-145-5p inhibitor+ Resatorvid groups. The treatments of different groups were similar to the first two parts of cell experiments. For the OGD 4.5h/R+si-MEG3+miR-145-5p inhibitors+ Resatorvid group, except si-MEG3 and miR-145-5p inhibitors transfection and OGD/R induction, cells were also pre-treated with resatorvid at the concentration of 100 nM.

OGD/R induction

The OGD/R was induced as preciously described (Belayev et al. 1996). In brief, HT22 cells were washed and cultured in sugar-free DMEM medium under specific conditions (37 °C, 1% O_2, 94% N_2, and 5% CO_2) for 2 h (OGD 2h/R) or 4.5 h (OGD 4.5h/R). This process induced the oxygen-glucose deprivation (OGD). After that, the medium was replaced with high-glucose DMEM and the cells were incubated in a normoxic incubator (37 °C, 95% air, 5% CO_2) for 48 h. This process stimulated the reperfusion. HT22 cells of the control group did not have to receive OGD induction.

Transfection

Small interfering RNA for MEG3 (si-MEG3), rno-miR-145-5p inhibitor (micrOFF miR-145-5p inhibitor), and their negative controls (siR NC and micrOFF inhibitor NC) were obtained from RIBOBIO. For rats and cells, the transfection was performed using Invivofectamine 3.0 (Invitrogen, Carlsbad, USA) and Lipofectamine 2000 Transfection Kit (Invitrogen, Carlsbad, USA) following the manufacturer's instructions, respectively.

2,3,7-Triphenyltetrazolium chloride (TTC) staining

48 h after reperfusion, rats were deeply anesthetized and their brains were quickly isolated, frozen and sliced into 2-mm-thick sections. Sections were then immersed in 2% TTC solution for 30 min at 37 °C and fixed with 4% Paraformaldehyde (PFA). The infarction volume of brains was calculated using Image-Pro Plus6 software (Media Cybernetics, Rockville, USA).

Real-time PCR

The extraction of total RNA was performed using the Trizol kit (Solarbio, Beijing, China). The concentration and purity of RNA were assessed using NanoDrop. The RNA was reverse transcripted with HiScript III 1 st Strand cDNA Synthesis Kit (+ gDNA wiper) (Vazyme, Nanjing, China). Real-time PCR was carried out using Maxima SYBR green/ROX PCR Master Mix (Thermo Scientific, Waltham, USA). The expression levels of MEG3, miR-145-5p, and TLR4 were normalized to the level of GAPDH or U6. Primer sequences were as follows: MEG3 forward: 5'-TGCCCATCTACAC CTCACG- 3', and reverse: 5'-AGCTGGCTGGTCAGTTC C- 3'; miR-145-5p forward: 5'-CGGTCCAGTTTTCCCA GGA- 3', and reverse: 5'-AGTGCAGGGTCCGAGGTAT T- 3'; TLR4 forward: 5'-TCCCTGCATAGAGGTAGTTC C- 3', and reverse: 5'-TCAAGGGGTTGAAGCTCAGA- 3'; GAPDH forward: 5'-CAGGAGAGTGTTTCCTCGTC C- 3', and reverse: 5'-TGCCGTGAGTGGAGTCATAC- 3'; U6 forward: 5'-TCGCTTCGGCAGCACA- 3', and reverse: 5'-AAATATGGAACGCTTCACGA- 3'.

TUNEL staining

TUNEL staining for HT22 cells and tissue samples was performed using the TUNEL Assay Kit - FITC (Abcam, Cambridge, UK) and TUNEL Assay Kit - HRP-DAB (Abcam, Cambridge, UK), respectively. For HT22 cell detection, cells were first fixed with ice-cold 70% (v/v) ethanol and stored at − 20 °C until use. Afterward, the cells were centrifuged at 300×g for 5 min to remove the ethanol and then washed twice with Wash Buffer. Subsequently, cells were incubated with DNA Labeling Solution for 60 min at 37 °C. Remove the DNA Labeling Solution by centrifuging and rinse the cells twice with Rinse Buffer. Finally, cells were incubated with Propidium Iodide/RNase A Solution for 30 min and observed under a microscope (Zeiss, Oberkochen, Germany). For tissue detection, the paraffin-embedded tissue sections were prepared and followed by rehydration, permeabilization, quenching, and equilibration. Then the sections were labeled with TdT enzyme. The labeling reaction was terminated, and the sections were blocked. After the final permeabilization, the sections were observed using a microscope (Zeiss, Oberkochen, Germany).

Western blot

Total proteins were isolated using RIPA protein lysate (Solarbio, Beijing, China), and the protein concentration

was determined using the BCA Protein Concentration Assay Kit (Solarbio, Beijing, China). The extracted proteins were denatured and separated by SDS-PAGE. Following the transfer of the proteins to the membrane, the membrane was blocked and incubated with primary antibodies (TLR4, NLRP3, Caspase-1, IL-1β, IL-18, GAPDH) (Invitrogen, Carlsbad, USA). After incubation, the membranes were incubated with secondary antibodies. The bands were visualized using Enhanced Chemiluminescence Kit (Bio-Rad Laboratories, Hercules, USA). Finally, the proteins were detected using Amersham Imager 600 (GE, Boston, USA).

Dual-luciferase reporter assay

The Starbase database was utilized to forecast the association between miR-145-5p and MEG3 or TLR4. The MEG3 -3'UTR and TLR4 -3'UTR fragments, which contain the anticipated binding site of miR-145, were inserted into the psi-CHECK2 vector to create wild-type recombinant luciferase reporter vector (WT-MEG3, WT-TLR4). The presumed binding sites were altered using the QuickChange targeted mutagenesis kit. The altered segments of MEG3 and TLR4 were introduced into the psi-CHECK2 vector to create mutant recombinant luciferase reporter vector (WUT-MEG3, WUT-TLR4). HEK293 T cells were transfected with each vector along with either a miR-145 mimic or a miR-NC using Lipofectamine 2000 (Invitrogen, Carlsbad, CA). After 48 h, the level of luciferase activity was determined using the Dual-Glo Luciferase Assay System (Promega, Madison, USA). Firefly luciferase activity was normalized to Renilla luciferase activity.

Statistical analysis

The experiment's data were presented as the mean ± standard deviation (SD), and data analysis and charting were performed using GraphPad Prism 10.0.0 software. The t-test was employed to assess the differences between the two conditions, while one-way analysis of variance (ANOVA) with Bonferroni's post-test was employed to compare the data across different groups. A p-value less than 0.05 was considered to be statistically significant.

Results

LncRNA MEG3 increasingly expressed in the rat model of MCAO/R

Previous research has demonstrated that LncRNA MEG3 is up-regulated and exacerbates cerebral CIRI (Zhao et al. 2023). To investigate the alterations in MEG3 during

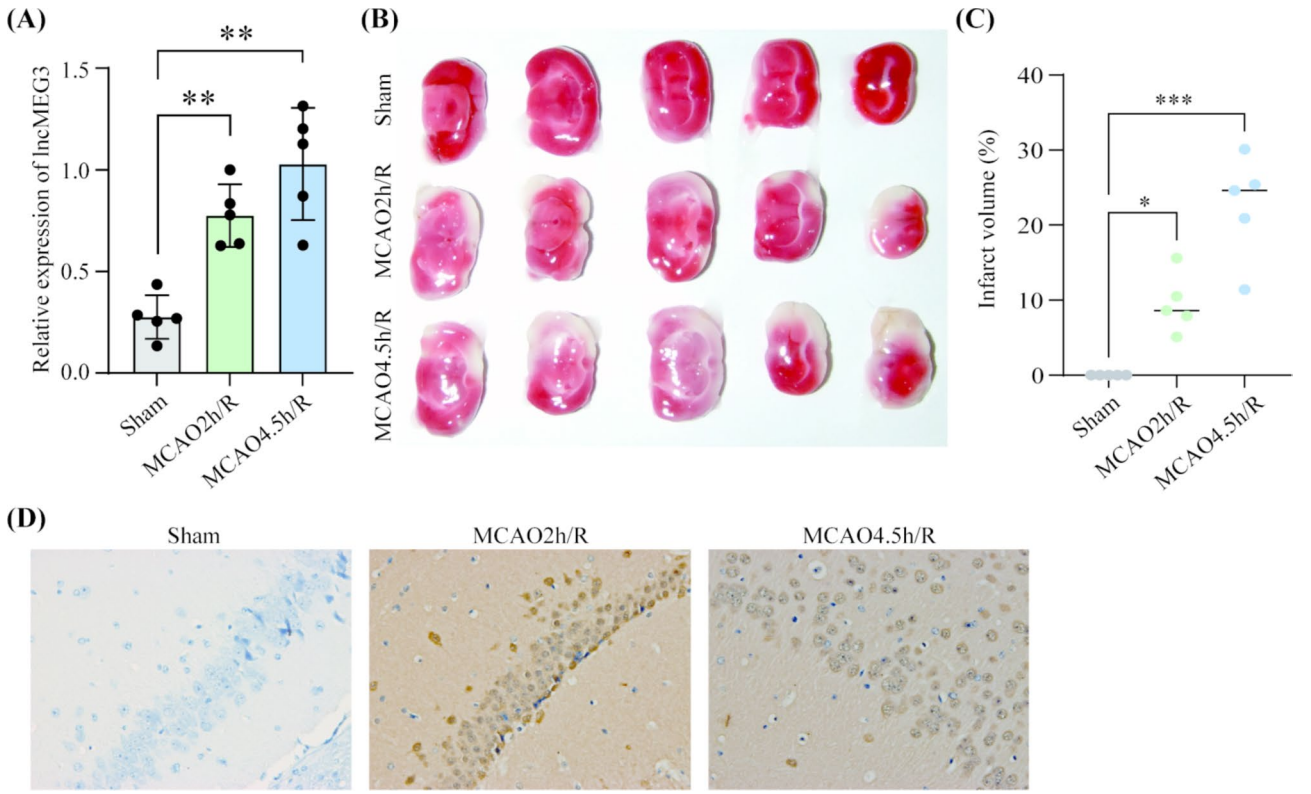

Fig. 1 LncRNA MEG3 increasingly expressed in the rat model of MCAO/R. (**A**) PCR of LncRNA MEG3 expression in rats. (**B**) TTC staining of brain sections. (**C**) Infract volume of MCAO/R rats. (**D**) TUNEL staining of brain sections. *$p < 0.05$, **$p < 0.01$, ***$p < 0.001$

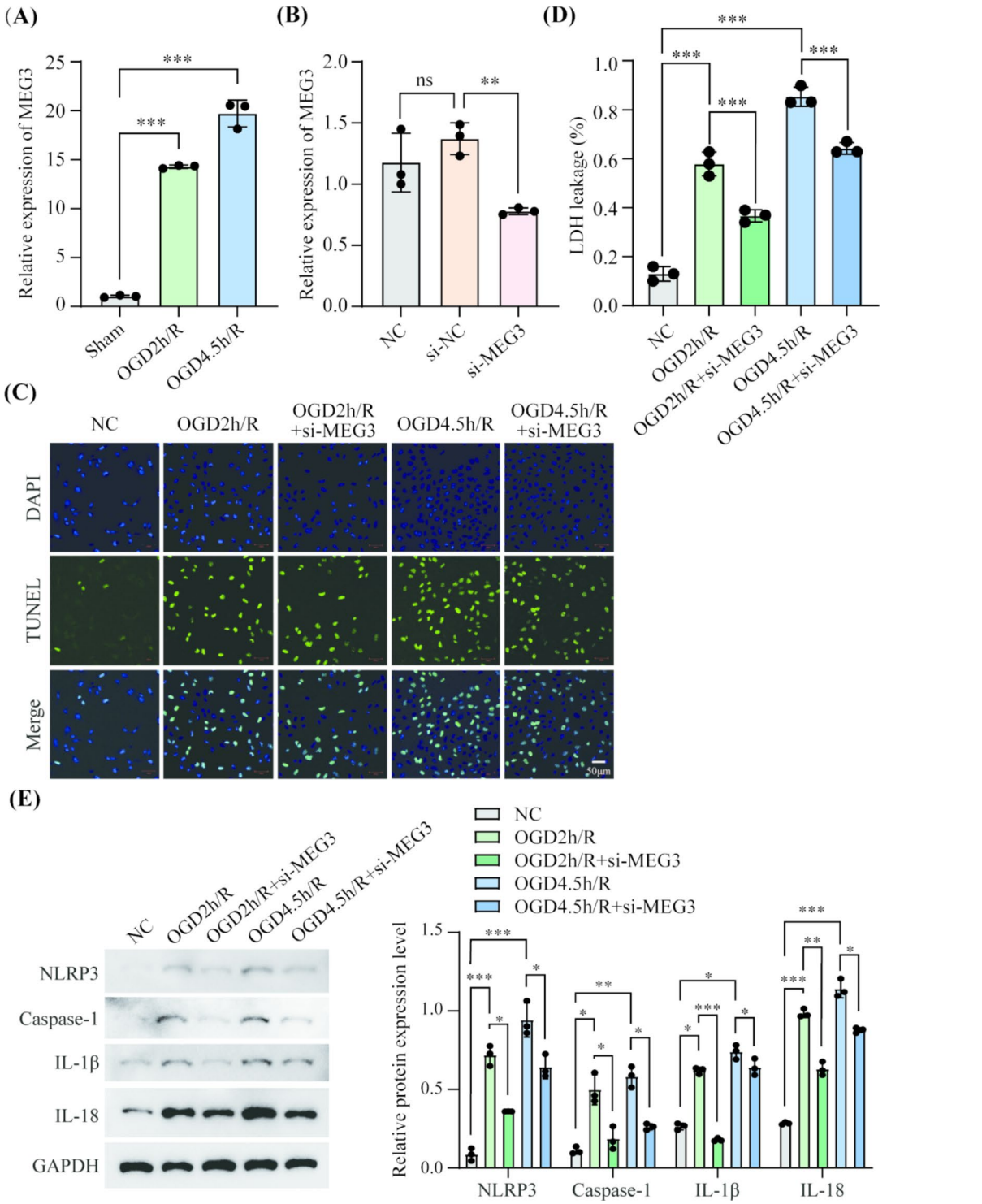

Fig. 2 Suppression of LncRNA MEG3 alleviated OGD/R-induced pyroptosis. (**A**) PCR detection of MEG3 in HT22 cells. (**B**) si-MEG3 transfection efficiency. (**C**) TUNEL staining of HT22 cells. (**D**) LDH determination of HT22 cells. (**E**) The differential protein expression of NLRP3, Caspase-1, IL-1β, and IL-18 in HT22 cells. $^{**}p < 0.01$, $^{***}p < 0.001$. ns: non-significant

MCAO/R, different rat models of MCAO/R were established. As shown in Fig. 1A, the expression of MEG3 was elevated in MCAO 2h/R and MCAO 4.5h/R group. Then, the brain injury and cell death were evaluated by TTC and TUNEL staining. Compared with the Sham group, severe infarction was observed in the MCAO/R groups, and the volume of infarcts and cell death increased with the increasing occlusion time (Fig. 1B-D).

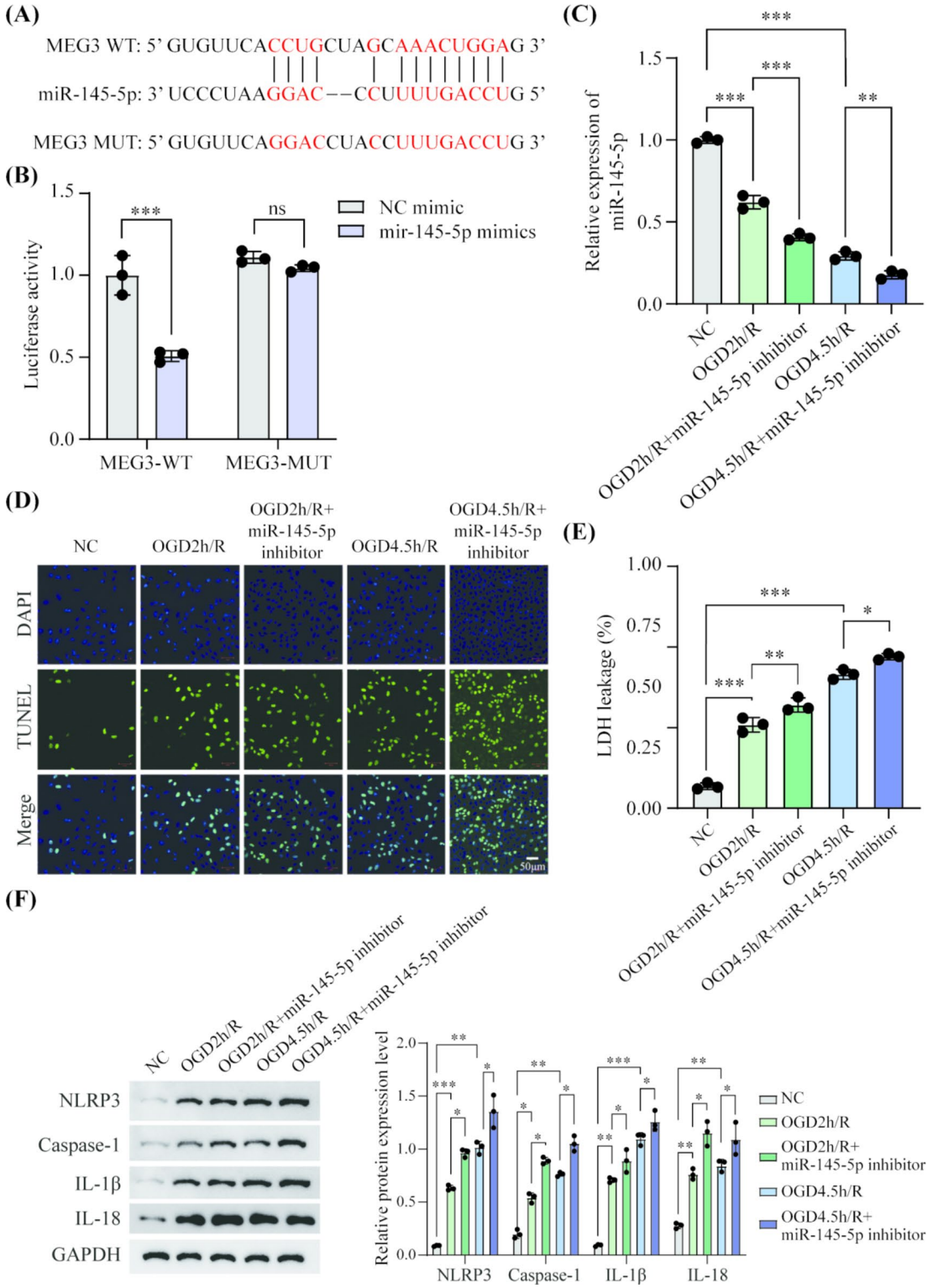

Fig. 3 LncRNA MEG3 aggravated OGD/R-induced pyroptosis by targeting miR-145-5p. (**A**) The inferred binding regions between miR-145-5p and MEG3. (**B**) Dual luciferase reporter assay of miR-145-5p and MEG3. (**C**) The differential mRNA expression level of miR-145-5p. (**D**) TUNEL staining of HT22 cells. (**E**) LDH determination of HT22 cells. (**F**) The expression level of pyroptosis-related proteins. *$p < 0.05$, **$p < 0.01$, ***$p < 0.001$. ns: non-significant

Suppression of LncRNA MEG3 alleviated OGD/R-induced pyroptosis

Investigations were conducted to examine the impacts and underlying processes of MEG3 on CIRI. The expression of LncRNA MEG3 in the HT22 cells suffered OGD/R was significantly increased (Fig. 2A). Transfection was conducted to knock down the expression of MEG3 in HT22 cells (Fig. 2B). As shown in TUNEL staining, OGD/R increased death rate of HT22 cells. Compared with the OGD 2h/R and OGD 4.5h/R group, MEG3 knockout (OGD 2h/R+si-MEG3 and OGD 4.5h/R+si-MEG3 group) remarkably reversed cell death induced by OGD/R (Fig. 2C). Moreover, the results of LDH detection suggested an up-regulation of LDH levels in OGD/R-treated cells, while MEG3 knockout counteracted the effect of OGD/R (Fig. 2D). Results above indicated that OGD/R induced TUNEL-positive and LDH-related cell death, which are also features of pyroptosis. The pyroptosis-related proteins were identified. The protein expression of NLRP3, Caspase-1, IL-1β, and IL-18 was enhanced by OGD/R treatment, indicating the involvement of pyroptosis in OGD/R. The knockdown of MEG3 reversed the increasing trends of these proteins (Fig. 2E).

LncRNA MEG3 aggravated OGD/R-induced pyroptosis by targeting miR-145-5p

Starbase (https://rnasysu.com/encori/) was used to screen for miRNAs that exhibit complementary base pairing with MEG3, and miR-145-5p was suggested as a potential target of MEG3 (Fig. 3A). The dual-luciferase reporter assay further confirmed the interaction between MEG3 and miR-145-5p (Fig. 3B). OGD/R inhibited the miR-145-5p expression in HT22 cells. Transfection of miR-145-5p inhibitor further reduced the expression of miR-145-5p in OGD/R-treated cells (Fig. 3C). Moreover, the transfection of miR-145-5p inhibitor promoted cell death and elevated LDH level induced by OGD/R (Fig. 3D-E). And the pyroptosis-related

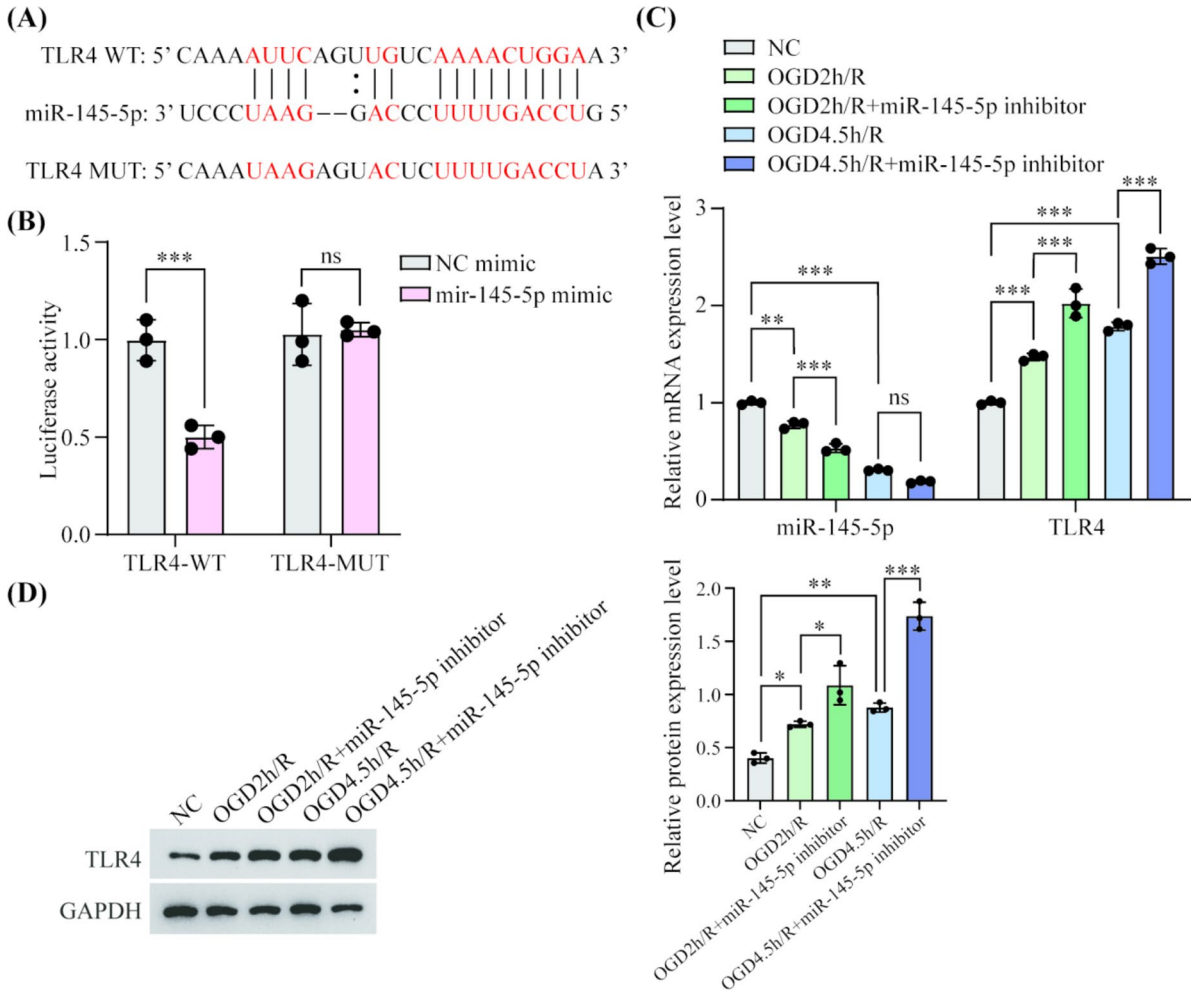

Fig. 4 miR-145-5p negatively regulates TLR4 to attenuate OGD/R-induced pyroptosis. (**A**) The inferred binding regions between miR-145-5p and TLR4. (**B**) Dual luciferase reporter assay of miR-145-5p and TLR4. (**C**) The differential mRNA expression level of miR-145-5P. (**D**) The expression level of pyroptosis-related proteins. $^{**}p < 0.01$, $^{***}p < 0.001$. ns: non-significant

protein was further enhanced by miR-145-5p inhibition (Fig. 3F). More experiments were conducted to confirm the interaction between MEG3 and miR-145-5p. Compared with the NC group, the expression of miR-145-5p was significantly inhibited by OGD 4.5h/R treatment, and the knockout of MEG3 reversed the effect. However, co-transfection of miR-145-5p inhibitor with si-MEG3 counteracted the impact of si-MEG3 (Supplement Fig. 1A). TUNEL staining was conducted to assess cell viability. As shown in Supplement Fig. 1B, transfection of miR-145-5p inhibitor against the effect of si-MEG3. The cell viability of OGD 4.5h/R+si-MEG3 group was higher than that of OGD 4.5h/R group, while the OGD 4.5h/R+si-MEG3 +miR-145-5p inhibitor group exhibited the highest cell death rate. The results of LDH detection revealed the same trend as the TUNEL staining. The transfection of miR-145-5p inhibitor against the inhibitory effect of si-MEG3 (Supplement Fig. 1C). Compared with the OGD 4.5h/R group, the expression of pyroptosis-related proteins was down-regulated in the OGD 4.5h/R+si-MEG3 group and up-regulated in the OGD 4.5h/R+si-MEG3+miR-145-5p inhibitor group (Supplement Fig. 1D). In conclusion, pyroptosis induced by OGD 4.5h/R was inhibited by MEG3 knockout. Inhibiting miR-145-5p expression counteracted this effect, suggesting that MEG3 exacerbated OGD/R-induced pyroptosis by targeting miR-145-5p.

miR-145-5p negatively regulates TLR4 to attenuate OGD/R-induced pyroptosis

To explore the potential downstream gene involved in the regulation of miR-145-5p on OGD/R-induced pyroptosis,

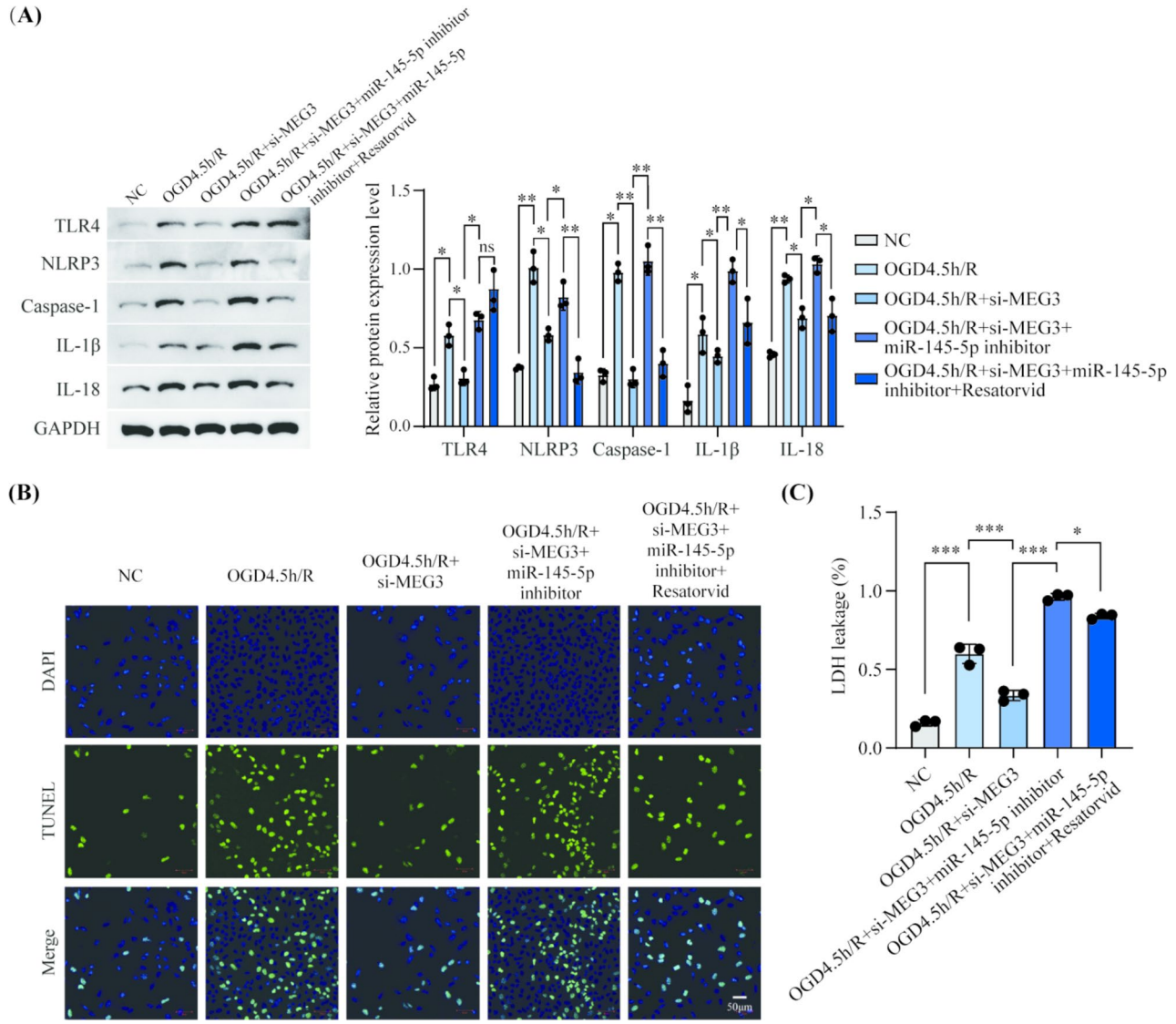

Fig. 5 LncRNA MEG3 aggravated pyroptosis by negatively regulating miR-145-5p/TLR4 axis in vitro. (**A**) The differential protein expression of pyroptosis-related proteins. (**B**) TUNEL staining of HT22 cells. (**C**) LDH detection of HT22 cells. *$p < 0.05$, ***$p < 0.001$

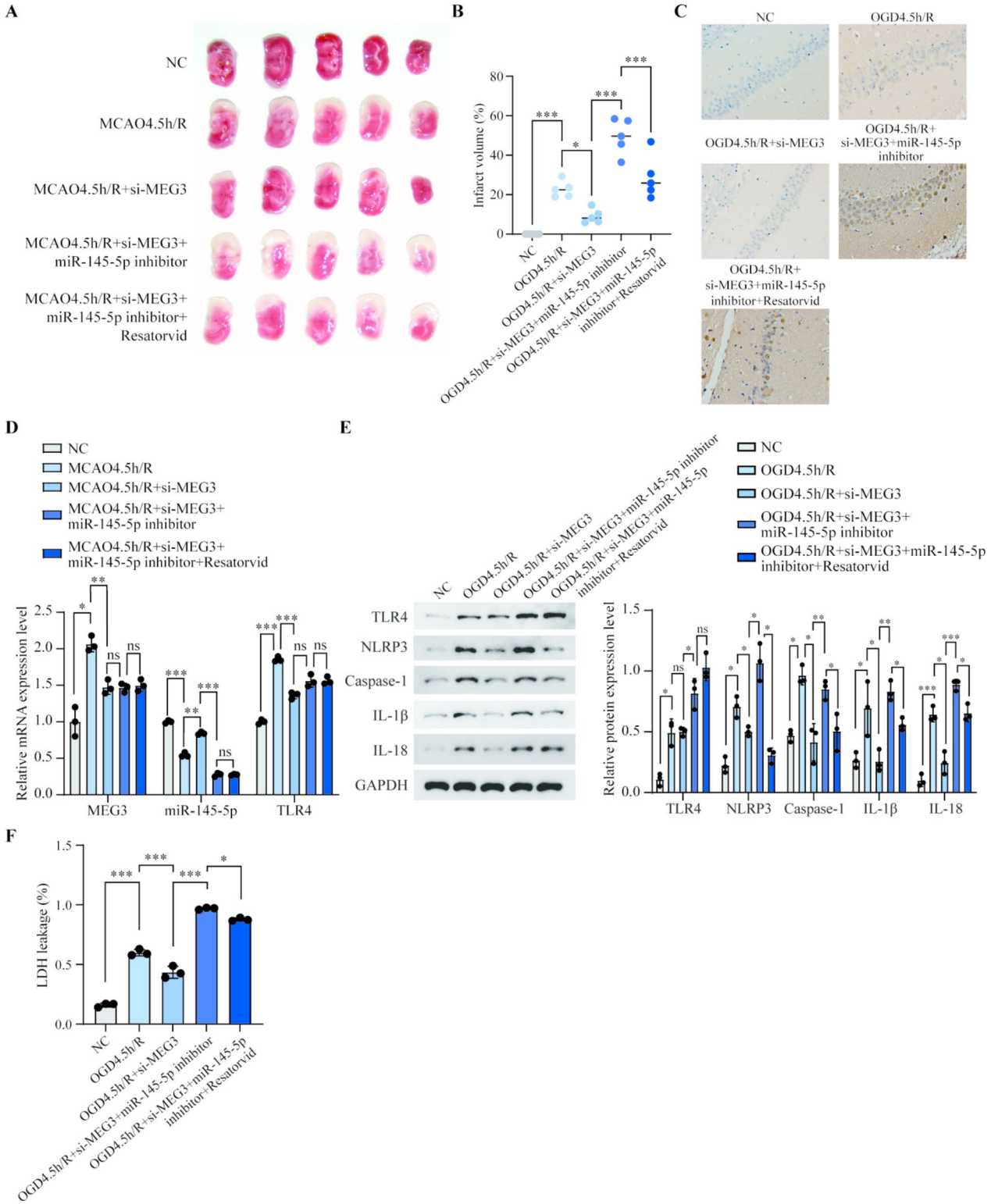

Fig. 6 LncRNA MEG3 aggravated pyroptosis by negatively regulating miR-145-5p/TLR4 axis in vivo. (**A**) TTC staining of rat brain sections. (**B**) Infract volume of MCAO/R rats. (**C**) TUNEL staining of rat brain sections. (**D**) The relative mRNA expression level MEG3, miR-145-5p, and TLR4 in rat brain tissue. (**E**) The differential protein expression of TLR4, NLRP3, Caspase-1, IL-1β and IL-18. (**F**) LDH content of rat brain tissue. *$p < 0.05$, **$p < 0.01$, ***$p < 0.001$. ns: non-significant Supplement Fig. 1. LncRNA MEG3 aggravated OGD/R-induced pyroptosis by targeting miR-145-5p (**A**) The differential mRNA expression level of miR-145-5P after co-transfection of si-MEG3 and miR-145-5p inhibitor. (**B**) TUNEL staining of co-transfected HT22 cells. (**C**) LDH determination of co-transfected HT22 cells. (**D**) The expression level of pyroptosis-related proteins in co-transfected HT22 cells. **$p < 0.01$, ***$p < 0.001$

the potential target genes were predicted. As shown in Fig. 4A, miR-145-5p had a sequence complementary to the region of TLR4. The dual-luciferase reporter assay further confirmed the interaction between TLR4 and miR-145-5p (Fig. 4B). Moreover, the differential expression of TLR4 and miR-145-5p was determined. In OGD/R-treated HT22 cells, the expression of miR-145-5p decreased, while the expression of TLR4 increased. Inhibition of miR-145-5p further aggravated this effect (Fig. 4C-D).

LncRNA MEG3 aggravated pyroptosis by negatively regulating miR-145-5p/TLR4 axis in vitro

si-MEG3, miR-145-5p, as well as a TLR4 inhibitor-Resatorvid were used for validate the involvement of miR-145-5p/TLR4 axis in OGD/R-induced pyroptosis. The si-MEG3 transfection inhibited OGD/R-induced up-regulation of TLR4, NLRP3, Caspase-1, IL-1β, and IL-18. While the transfection of miR-145-5p inhibitor counteracted the effect of si-MEG3. The effects of joint application of si-MEG3, miR-145-5p, and Resatorvid were also confirmed. Compared with the OGD 4.5h/R+si-MEG3+miR-145 inhibitor group, the OGD 4.5h/R+si-MEG3 +miR-145 inhibitor+ Resatorvid group exhibited a similar TLR4 level but lower levels of NLRP3, Caspase-1, IL-1β, and IL-18 (Fig. 5A). Compared to the OGD 4.5h/R+si-MEG3+miR-145-5p inhibitor group, the use of Resatorvid decreased cell death rate and intracellular LDH level (Fig. 5B-C).

LncRNA MEG3 aggravated pyroptosis by negatively regulating miR-145-5p/TLR4 axis in vivo

The involvement of miR-145-5p/TLR4 axis in MCAO/R-induced pyroptosis was also confirmed. The infarction volume of different groups was shown in Fig. 6A-B. MCAO/R significantly induced brain injury, and transfection of si-MEG3 reduced the volume of infarction. In addition, transfection of miR-145-5p inhibitor counteracted the effect of si-MEG3, while the TLR4 inhibitor Resatorvid counteracted the effect of miR-145-5p inhibitor. The volume of infarction of MCAO/R+si-MEG3 +miR-145-5p inhibitor group was larger than that of MCAO/R+si-MEG3+miR-145-5p inhibitor+ Resatorvid group. TUNEL staining of rat brain sections showed same trend as the infarction volume. miR-145-5p inhibitor reversed the effect of si-MEG3, while Resatorvid counteracted the effect of miR-145-5p inhibitor (Fig. 6C). The mRNA expression level of miR-145-5p and TLR4 was increased in rat brain tissue after MCAO/R treatment. The knockdown of MEG3 reversed MCAO/R. And the co-transfection of si-MEG3 and miR-145-5p inhibitor inhibited miR-145-5p expression and elevated TLR4 expression when compared to the MCAO/R +si-MEG3 group. The use of Resatorvid showed no effect on the mRNA expression of MEG3, miR-145-5p and TLR4 when compared to the MCAO/R+si-MEG3+miR-145-5p inhibitor group (Fig. 6D). The protein expression level of TLR4, NLRP3, Caspase-1, IL-1β, and IL-18 was enhanced after MCAO/R treatment. si-MEG3 inhibited the elevation of these pyroptosis-related protein. miR-145-5p inhibitor against the effect of si-MEG3. Resatorvid reversed the effect of miR-145-5p inhibitor, inhibited the expression of NLRP3, Caspase-1, IL-1β and IL-18 (Fig. 6E). The LDH content of rat brain tissue was also assessed. Transfection of si-MEG3 inhibited the MCAO/R-induced LDH production, while transfection of miR-145-5p inhibitor against the effect of si-MEG3. As the use of Resatorvid impaired the effect of miR-145-5p inhibitor, the group of MCAO/R+si-MEG3+miR-145-5p inhibitor+ Resatorvid exhibited lower LDH level than that of MCAO/R+si-MEG3+miR-145-5p inhibitor group (Fig. 6F).

Discussion

This study confirmed that the elevated expression of LncRNA MEG3 during CIRI. There was a strong correlation between the severity of CIRI and the duration of reperfusion. In the MCAO/R rat model and OGD/R cell model, MEG3 contributes to pyroptosis by regulating the miR-145-5p/TLR4 axis. The knockdown of MEG3 reduced the expression of NLRP3, Caspase-1, IL-1β, and IL-18, thereby preventing pyroptosis in brain tissues and cells. However, inhibition of miR-145-5p reversed the effect of MEG3 knockdown and promoted pyroptosis, suggesting that MEG3 acts as a ceRNA to negatively regulate miR-145-5p expression. Furthermore, resatorvid, the inhibitor of TLR4, counteracted the effect of miR-145-5p inhibitor and inhibited pyroptosis. This indicated that TLR4 was the downstream of miR-145-5p, and MEG3 exacerbated pyroptosis by regulating miR-145-5p/TLR4 axis.

Different kinds of cell death and cell dysfunctions are involved in CIRI. Previous studies have identified that apoptosis, necroptosis, ferroptosis, and autophagy are implicated in CIRI (Li et al. 2019, 2022a; Tuo et al. 2022; Xu et al. 2023). Though treatments based on these cell death patterns has been made some progress, the outcomes are still far from satisfactory. Fortunately. more and more studies have reported targeting CIRI-related pyroptosis providing promising and effective approaches to alleviating CIRI (Zheng et al. 2022). An increasing number of studies have suggested that lncRNA is capable of mediating pyroptosis (Hu et al. 2023; Li et al. 2022b; Sun et al. 2021), and lncRNA-mediated pyroptosis has significance in various diseases, including diabetes, cardiovascular diseases, cancer, etc. (Meng et

al. 2022; Wang et al. 2023). Researches based on lncRNA MEG3 has found that it regulates pyroptosis in triple-negative breast cancer, testicular ischemia-reperfusion injury, myocardial infarction, and chronic obstructive pulmonary disease (Ning et al. 2021; Qin et al. 2023; Wang et al. 2024; Yan et al. 2021). Our study is the first to confirm that MEG3 regulates pyroptosis to exacerbate CIRI.

miR-145-5p plays a significant role in CIRI. A miRNA microarray of MCAO/R rat cortex samples was performed, and miR-145-5p was found to regulate Nurr1 directly through its 3′UTR. Transfection of anti-miR-145-5p increased the expression of Nurr1, protecting rats from ischemia-induced infarct volume and inflammation injury (Xie et al. 2017). Another study had reported that in the MCAO/R mouse model and OGD/R microglia cell, lncRNA SNHG14 was highly expressed, and it promotes microglia activation. The knock down of SNHG14 up-regulated the expression of miR-145-5p, inhibited the activation of MCs in cerebral infarction (Qi et al. 2017). Our research findings were consistent with the results showing that miR-145-5p directly interacts with MEG3 through its 3′UTR.

Studies have reported that TLR4 was targeted by miR-145-5p (Jiang and Zhang 2021; Yu et al. 2019). In synovium-derived mesenchymal stem cells, miR-145-5p restrains chondrogenesis of SMSCs by suppressing TLR4 (Wu et al. 2022a). In malignant melanoma, miR-145-5p inhibits tumor occurrence and metastasis by regulating TLR4 (Jin et al. 2019). In cardiomyocytes, miR-145-5p against the hypoxia/reoxygenation-induced pyroptosis by inhibiting TLR4 expression (Wei and Zhao 2022). In this study, it was found that TLR4 functions as the downstream target of miR-145-5p and a direct inducer of lncRNA MEG3-related pyroptosis during CIRI. Numerous studies have demonstrated the significant involvement of the toll-like receptors (TLRs) pathway, which serves as a pattern-recognition receptor for innate immune responses. TLR4 plays a crucial role as a mediator in the neuroinflammatory cascade. It activates the p65 subunit of the downstream NF-κB pathway, leading to the promotion of the transcription of NLRP3 components. This, in turn, regulates the release of downstream inflammatory mediators as part of an inflammatory response and induces pyroptosis (Silveira et al. 2016). The NLRP3 inflammasome (composed of NLRP3, ASC and procassase-1) participates in the process of pyroptosis. Studies have found that pyroptosis mediated by NLRP3 inflammasome play a vital role in the pathological process of CIRI and confirmed that inhibition of NLRP3 inflammasome can improve neural function and reduce the volume of infarction (Long et al. 2023).

Extensive research has demonstrated that both miRNAs and lncRNAs play significant roles in CIRI through mechanisms such as pyroptosis and oxidative stress, highlighting their potential as promising therapeutic targets. Recently, stem cell-derived exosomes and nano-drug delivery systems have been shown to effectively alleviate CIRI (Zhang et al. 2023; Zhu et al. 2023). In these advanced therapeutic approaches, miRNAs and lncRNAs serve as direct mediators, driving the observed therapeutic effects. It has been reported that exosomes derived from mesenchymal stem cells (MSCs) reduce oxidative stress through the miR- 486 - 5p/PTEN axis, thereby mitigating CIRI (Zhu et al. 2024). Additionally, bone marrow mesenchymal stem cell-derived exosomal lncRNA KLF3-AS1 has been shown to improve CIRI via the miR- 206/USP22 axis (Xie et al. 2023). Furthermore, lncRNAs and miRNAs can also be delivered to the lesion site through exosomes or nano-drug delivery systems. This study investigated the role of MEG3 in CIRI-induced neuronal injury by exploring its interaction with miR-145-5p to regulate pyroptosis. The findings suggest that both MEG3 and miR-145-5p are potential therapeutic targets. In the future, therapies targeting MEG3 or miR-145-5p, such as siRNA or miRNA mimics, combined with advanced delivery technologies like exosomes or nano-delivery systems, could offer novel treatment strategies for CIRI patients.

Our study has validated that MEG3 enhances pyroptosis through the miR-145-5p/TLR4/NLRP3 axis, consequently mitigating CIRI-induced brain damage. Therefore, based on our data analysis, it can be inferred that MEG3 has the potential to serve as a target for the treatment of CIRI injury. Nevertheless, certain constraints may be present in the existing research. The impact of miR-145-5p overexpression on the MCAO/R and OGD/R models was not observed. On the contrary, other types of cell death related to CIRI was not implicated in this investigation. Hence, additional efforts are required to delve deeper into the molecular mechanism of CIRI. It is essential to present more comprehensive scientific evidence.

Supplementary Information The online version contains supplementary material available at https://doi.org/10.1007/s11011-025-01613-x.

Author contributions Lei Li conceived and designed the experiments; Hao Zha, Wei Miao carried out the construction of the model of CIRI in animals and cells and instructed the animal experiments; Chunyan Li and Aimei Wang instructed the cell experiments and completed the cell cultures; Shiyuan Qin, Shuang Gao and Lingli Sheng collected and analyzed the data. Lei Li wrote the manuscript; Ying Wang corrected the manuscript and revised the language. All authors contributed to the article and approved the submitted version, and all authors read and agreed to the published version of the manuscript.

Funding This work was supported by National Natural Science Foundation of China (Grant No. 82060233); Yunnan Provincial Department of Science and Technology Basic Research Program (Grant No.202101 AT070229); Yunnan Provincial Reserve Program for Young and Middle-aged Academic and Technical Leaders (No.202305 AC160055).

Data availability The datasets used or analyzed during the current study are available from the corresponding author on reasonable request.

Declarations

Ethics approval and consent to participate This study was conducted in accordance with the guiding principles of the Declaration of Helsinki and was approved by the Ethics Committee of the Second Affiliated Hospital of Kunming Medical University (protocol code: Audit-PJ-Ko- 2022 - 124, approval date: May 5, 2022) and the Laboratory Animal Ethics Committee of Yunnan Luoyu Biotechnology Co Ltd (protocol code: SL20230410, Approval date: April 5, 2023).

Consent for publication Not applicable.

Competing interests The authors declare no competing interests.

References

Bailey EL, Smith C, Sudlow CL, Wardlaw JM (2012) Pathology of lacunar ischemic stroke in humans–a systematic review. Brain Pathol 22:583–591

Belayev L, Alonso OF, Busto R, Zhao W, Ginsberg MD (1996) Middle cerebral artery occlusion in the rat by intraluminal suture. Neurological and pathological evaluation of an improved model. Stroke 27:1616–1622 discussion 1623

Chen R, Zhu H, Wang Z, Zhang Y, Wang J, Huang Y, Gu L, Li C, Xiong X, Jian Z (2023) Targeting microglia/macrophages Notch1 protects neurons from pyroptosis in ischemic stroke. Brain Sci 13:1657

Cookson BT, Brennan MA (2001) Pro-inflammatory programmed cell death. Trends Microbiol 9:113–114

Hu B, Chen W, Zhong Y, Tuo Q (2023) The role of lncRNA-mediated pyroptosis in cardiovascular diseases. Front Cardiovasc Med 10:1217985

Jean WC, Spellman SR, Nussbaum ES, Low WC (1998) Reperfusion injury after focal cerebral ischemia: the role of inflammation and the therapeutic horizon. Neurosurgery 43:1382–1396 discussion 1396-7

Jiang Z, Zhang J (2021) Mesenchymal stem cell-derived exosomes containing miR-145-5p reduce inflammation in spinal cord injury by regulating the TLR4/NF-kappaB signaling pathway. Cell Cycle 20:993–1009

Jin C, Wang A, Liu L, Wang G, Li G, Han Z (2019) miR-145-5p inhibits tumor occurrence and metastasis through the NF-kappaB signaling pathway by targeting TLR4 in malignant melanoma. J Cell Biochem 120:11115–11126

Li J, Zhang J, Zhang Y, Wang Z, Song Y, Wei S, He M, You S, Jia J, Cheng J (2019) TRAF2 protects against cerebral ischemia-induced brain injury by suppressing necroptosis. Cell Death Dis 10:328

Li T, Luo Y, Zhang P, Guo S, Sun H, Yan D, Liu X, Yang B (2020) LncRNA MEG3 regulates microglial polarization through KLF4 to affect cerebral ischemia-reperfusion injury. J Appl Physiol (1985) 129:1460–1467

Li M, Ning J, Huang H, Jiang S, Zhuo D (2022a) Allicin protects against renal ischemia-reperfusion injury by attenuating oxidative stress and apoptosis. Int Urol Nephrol 54:1761–1768

Li X, Bai C, Wang H, Wan T, Li Y (2022b) LncRNA MEG3 regulates autophagy and pyroptosis via FOXO1 in pancreatic beta-cells. Cell Signal 92:110247

Liang J, Wang Q, Li JQ, Guo T, Yu D (2020) Long non-coding RNA MEG3 promotes cerebral ischemia-reperfusion injury through increasing pyroptosis by targeting miR-485/AIM2 axis. Exp Neurol 325:113139

Liu X, Hou L, Huang W, Gao Y, Lv X, Tang J (2016) The mechanism of long Non-coding RNA MEG3 for neurons apoptosis caused by hypoxia: mediated by miR-181b-12/15-LOX signaling pathway. Front Cell Neurosci 10:201

Long JX, Tian MZ, Chen XY, Yu HH, Ding H, Liu F, Du K (2023) The role of NLRP3 inflammasome-mediated pyroptosis in ischemic stroke and the intervention of traditional Chinese medicine. Front Pharmacol 14:1151196

Meng J, Ding T, Chen Y, Long T, Xu Q, Lian W, Liu W (2021) LncRNA-Meg3 promotes Nlrp3-mediated microglial inflammation by targeting miR-7a-5p. Int Immunopharmacol 90:107141

Meng L, Lin H, Huang X, Weng J, Peng F, Wu S (2022) METTL14 suppresses pyroptosis and diabetic cardiomyopathy by downregulating TINCR LncRNA. Cell Death Dis 13:38

Ning JZ, He KX, Cheng F, Li W, Yu WM, Li HY, Rao T, Ruan Y (2021) Long Non-coding RNA MEG3 promotes pyroptosis in testicular Ischemia-Reperfusion injury by targeting MiR-29a to modulate PTEN expression. Front Cell Dev Biol 9:671613

Preethi KA, Sekar D (2021) Dietary MicroRNAs: current status and perspective in food science. J Food Biochem 45(7):e13827

Qi X, Shao M, Sun H, Shen Y, Meng D, Huo W (2017) Long non-coding RNA SNHG14 promotes microglia activation by regulating miR-145-5p/PLA2G4A in cerebral infarction. Neuroscience 348:98–106

Qin C, Wang T, Qian N, Liu J, Xi R, Zou Q, Liu H, Niu X (2023) Epigallocatechin gallate prevents cardiomyocytes from pyroptosis through LncRNA MEG3/TAF15/AIM2 axis in myocardial infarction. Chin Med 18:160

Quek XC, Thomson DW, Maag JL, Bartonicek N, Signal B, Clark MB, Gloss BS, Dinger ME (2015) LncRNAdb v2.0: expanding the reference database for functional long noncoding RNAs. Nucleic Acids Res 43:D168–D173

Selvakumar SC, Preethi KA, Sekar D (2023) MicroRNAs as important players in regulating cancer through PTEN/PI3K/AKT signalling pathways. Biochim Biophys Acta Rev Cancer 1878(3):188904

Selvakumar SC, Preethi KA, Sekar D (2024) MicroRNA-510-3p regulated vascular dysfunction in preeclampsia by targeting vascular endothelial growth factor A (VEGFA) and its signaling axis. Placenta 153:31–52

Shao BZ, Xu ZQ, Han BZ, Su DF, Liu C (2015) NLRP3 inflammasome and its inhibitors: a review. Front Pharmacol 6:262

Shi Q, Li Y, Li S, Jin L, Lai H, Wu Y, Cai Z, Zhu M, Li Q, Li Y, Wang J, Liu Y, Wu Z, Song E, Liu Q (2020) LncRNA DILA1 inhibits Cyclin D1 degradation and contributes to Tamoxifen resistance in breast cancer. Nat Commun 11:5513

Shi S, Zhang C, Liu J (2023) TIMP2 facilitates CIRI through activating NLRP3-mediated pyroptosis. Aging 15:3635–3643

Shuman S (2020) Transcriptional interference at tandem LncRNA and protein-coding genes: an emerging theme in regulation of cellular nutrient homeostasis. Nucleic Acids Res 48:8243–8254

Silveira LS, Antunes Bde M, Minari AL, Dos Santos RV, Neto JC, Lira FS (2016) Macrophage polarization: implications on metabolic diseases and the role of exercise. Crit Rev Eukaryot Gene Expr 26:115–132

Sun J, Mao S, Ji W (2021) LncRNA H19 activates cell pyroptosis via the miR-22-3p/NLRP3 axis in pneumonia. Am J Transl Res 13:11384–11398

Tu X, Zhang H, Chen S, Ding YH, Wu X, Liang R, Shi SS (2022) LncRNA CEBPA-AS1 alleviates cerebral ischemia-reperfusion injury by sponging miR-340-5p regulating APPL1/LKB1/AMPK pathway. FASEB J 36:e22075

Tuo QZ, Liu Y, Xiang Z, Yan HF, Zou T, Shu Y, Ding XL, Zou JJ, Xu S, Tang F, Gong YQ, Li XL, Guo YJ, Zheng ZY, Deng AP, Yang ZZ, Li WJ, Zhang ST, Ayton S, Bush AI, Xu H, Dai L, Dong B, Lei P (2022) Thrombin induces ACSL4-dependent ferroptosis during cerebral ischemia/reperfusion. Signal Transduct Target Ther 7:59

Wang Y, Ge P, Zhu Y (2013) TLR2 and TLR4 in the brain injury caused by cerebral ischemia and reperfusion. Mediators Inflamm 2013:124614

Wang P, Wang Z, Zhu L, Sun Y, Castellano L, Stebbing J, Yu Z, Peng L (2023) A pyroptosis-related LncRNA signature in bladder cancer. Cancer Med 12:6348–6364

Wang L, Yu Q, Xiao J, Chen Q, Fang M, Zhao H (2024) Cigarette smoke Extract-Treated mouse airway epithelial Cells-Derived Exosomal LncRNA MEG3 promotes M1 macrophage polarization and pyroptosis in chronic obstructive pulmonary disease by upregulating TREM-1 via m(6)A methylation. Immune Netw 24:e3

Wei L, Zhao D (2022) M2 macrophage-derived Exosomal miR-145-5p protects against the hypoxia/reoxygenation-induced pyroptosis of cardiomyocytes by inhibiting TLR4 expression. Ann Transl Med 10:1376

Winters L, Winters T, Gorup D, Mitrecic D, Curlin M, Kriz J, Gajovic S (2013) Expression analysis of genes involved in TLR2-related signaling pathway: inflammation and apoptosis after ischemic brain injury. Neuroscience 238:87–96

Wu M, Liu F, Yan L, Huang R, Hu R, Zhu J, Li S, Long C (2022a) MiR-145-5p restrains chondrogenic differentiation of synovium-derived mesenchymal stem cells by suppressing TLR4. Nucleosides Nucleotides Nucleic Acids 41:625–642

Wu XS, Wang F, Li HF, Hu YP, Jiang L, Zhang F, Li ML, Wang XA, Jin YP, Zhang YJ, Lu W, Wu WG, Shu YJ, Weng H, Cao Y, Bao RF, Liang HB, Wang Z, Zhang YC, Gong W, Zheng L, Sun SH, Liu YB (2022b) LncRNA-PAGBC acts as a MicroRNA sponge and promotes gallbladder tumorigenesis. EMBO Rep 23:e55711

Xiang Y, Zhang Y, Xia Y, Zhao H, Liu A, Chen Y (2020) LncRNA MEG3 targeting miR-424-5p via MAPK signaling pathway mediates neuronal apoptosis in ischemic stroke. Aging 12:3156–3174

Xie X, Peng L, Zhu J, Zhou Y, Li L, Chen Y, Yu S, Zhao Y (2017) miR-145-5p/Nurr1/TNF-alpha Signaling-Induced microglia activation regulates neuron injury of acute cerebral ischemic/reperfusion in rats. Front Mol Neurosci 10:383

Xie X, Cao Y, Dai L, Zhou D (2023) Bone marrow mesenchymal stem cell-derived Exosomal LncRNA KLF3-AS1 stabilizes Sirt1 protein to improve cerebral ischemia/reperfusion injury via miR-206/USP22 axis. Mol Med 29:3

Xiong W, Qu Y, Chen H, Qian J (2019) Insight into long noncoding RNA-miRNA-mRNA axes in myocardial ischemia-reperfusion injury: the implications for mechanism and therapy. Epigenomics 11:1733–1748

Xu Q, Guohui M, Li D, Bai F, Fang J, Zhang G, Xing Y, Zhou J, Guo Y, Kan Y (2021) LncRNA C2dat2 facilitates autophagy and apoptosis via the miR-30d-5p/DDIT4/mTOR axis in cerebral ischemia-reperfusion injury. Aging 13:11315–11335

Xu S, Huang P, Yang J, Du H, Wan H, He Y (2023) Calycosin alleviates cerebral ischemia/reperfusion injury by repressing autophagy via STAT3/FOXO3a signaling pathway. Phytomedicine 115:154845

Yan H, Luo B, Wu X, Guan F, Yu X, Zhao L, Ke X, Wu J, Yuan J (2021) Cisplatin induces pyroptosis via activation of MEG3/NLRP3/caspase-1/GSDMD pathway in Triple-Negative breast Cancer. Int J Biol Sci 17:2606–2621

Yao L, Peng P, Ding T, Yi J, Liang J (2024) m(6)A-Induced LncRNA MEG3 promotes cerebral Ischemia-Reperfusion injury via modulating oxidative stress and mitochondrial dysfunction by hnRNPA1/Sirt2 Axis. Mol Neurobiol 61:6893–6908

Yu YL, Yu G, Ding ZY, Li SJ, Fang QZ (2019) Overexpression of miR-145-5p alleviated LPS-induced acute lung injury. J Biol Regul Homeost Agents 33:1063–1072

Yu J, Zhong B, Xiao Q, Du L, Hou Y, Sun HS, Lu JJ, Chen X (2020) Induction of programmed necrosis: A novel anti-cancer strategy for natural compounds. Pharmacol Ther 214:107593

Zhang R, Mao W, Niu L, Bao W, Wang Y, Wang Y, Zhu Y, Yang Z, Chen J, Dong J, Cai M, Yuan Z, Song H, Li G, Zhang M, Xiong N, Wei J, Dong Z (2023) NSC-derived exosomes enhance therapeutic effects of NSC transplantation on cerebral ischemia in mice. Elife 12:e84493

Zhao Y, Liu Y, Zhang Q, Liu H, Xu J (2023) The mechanism underlying the regulation of long Non-coding RNA MEG3 in cerebral ischemic stroke. Cell Mol Neurobiol 43:69–78

Zheng Y, Xu X, Chi F, Cong N (2022) Pyroptosis: a newly discovered therapeutic target for Ischemia-Reperfusion injury. Biomolecules 12:1625

Zhu Y, Rowley MJ, Bohmdorfer G, Wierzbicki AT (2013) A SWI/SNF chromatin-remodeling complex acts in noncoding RNA-mediated transcriptional Silencing. Mol Cell 49:298–309

Zhu ZH, Jia F, Ahmed W, Zhang GL, Wang H, Lin CQ, Chen WH, Chen LK (2023) Neural stem cell-derived exosome as a nano-sized carrier for BDNF delivery to a rat model of ischemic stroke. Neural Regen Res 18:404–409

Zhu G, Jiang L, Tan K, Li Y, Hu M, Zhang S, Liu Z, Li L (2024) MSCs-derived exosomes containing miR-486-5p attenuate cerebral ischemia and reperfusion (I/R) injury. Gene 906:148262

Authors and Affiliations

Lei Li[1] · Hao Zha[2] · Wei Miao[1] · Chunyan Li[1] · Aimei Wang[1] · Shiyuan Qin[1] · Shuang Gao[1] · Lingli Sheng[3] · Ying Wang[1]

✉ Ying Wang
wangying@kmmu.edu.cn

[1] Department of Neurology, The Second Affiliated Hospital of Kunming Medical University, No. 374, Dianmian Avenue, Wuhua District, Kunming 650032, Yunnan, China

[2] Department of Reproductive Medicine, The Second Affiliated Hospital of Kunming Medical University, Kunming 650032, China

[3] Department of Geriatrics, Baoshan People's Hospital, Baoshan 678000, China